RHEUMATOLOGY

Original article

doi:10.1093/rheumatology/kex234

# Quantitative measurement of $^{18}$F-FDG PET/CT uptake reflects the expansion of circulating plasmablasts in IgG4-related disease

**Alvise Berti[1,2,*], Emanuel Della-Torre[1,2,*], Francesca Gallivanone[3], Carla Canevari[4], Raffaella Milani[5], Marco Lanzillotta[1,2], Corrado Campochiaro[1,2], Giuseppe Alvise Ramirez[1,2], Emanuele Bozzalla Cassione[1,2], Enrica Bozzolo[2], Federica Pedica[6], Isabella Castiglioni[3], Paolo Giorgio Arcidiacono[7], Gianpaolo Balzano[8], Massimo Falconi[2,4,8], Luigi Gianolli and Lorenzo Dagna[1,2]**

## Abstract

**Objective.** [$^{18}$F]Fluorodeoxyglucose ($^{18}$F-FDG) PET/CT is increasingly used to assess organ involvement and response to treatment in IgG4-related disease (IgG4-RD), but clear correlations between $^{18}$F-FDG uptake and disease activity have not been established yet. We aimed to correlate the intensity and distribution of $^{18}$F-FDG uptake with validated clinical, serological and immunological parameters of IgG4-RD activity.

**Methods**. Twenty patients with active IgG4-RD underwent a baseline $^{18}$F-FDG PET/CT. Ten patients repeated $^{18}$F-FDG PET/CT after immunosuppressive treatments. $^{18}$F-FDG tissue uptake was measured using the standardized uptake value corrected for the partial volume effect (PVC-SUV) and the total lesion glycolysis (TLG) with ($TLG_{tot+ln}$) and without ($TLG_{tot-ln}$) lymph nodes. Disease activity was assessed by means of clinical parameters [IgG4-RD Responder Index (RI)], serological (ESR and CRP) and immunological (serum IgG4 and circulating plasmablasts) biomarkers. The enhanced liver fibrosis score was exploited as a biomarker for fibroblast activation.

**Results.** Thirteen (65%) patients had two or more organs affected by IgG4-RD. All patients had active IgG4-RD as defined by a median IgG4-RD RI value of 9 (range 6–15; normal $< 3$). Serum IgG4 and plasmablasts were elevated in 85% of patients. Circulating plasmablasts positively correlated with PVC-SUV ($P = 0.027$), inversely correlated with $TLG_{tot-ln}$ ($P = 0.023$) and did not correlate with $TLG_{tot+ln}$ ($P > 0.05$). No statistically significant correlation was found between PVC-SUV or TLG and IgG4-RD RI, ESR, CRP, serum IgG4 or enhanced liver fibrosis score ($P > 0.05$). Clinical response to immunosuppressive therapies was associated with a consensual reduction of circulating plasmablasts, PVC-SUV, $TLG_{tot+ln}$ and $TLG_{tot-ln}$ values ($P < 0.05$ for all comparisons).

**Conclusions.** $^{18}$F-FDG uptake of IgG4-RD lesions reflects immunological perturbations of the B cell compartment rather than fibroblast activation and extracellular matrix deposition. Conventional biomarkers of disease activity, namely IgG4-RD RI, ESR, CRP and serum IgG4 levels, do not appear to correlate with the radiometabolic activity of IgG4-RD lesions. In light of our results PET/CT represents a reliable instrument for assessing IgG4-RD activity, although lymph-node uptake deserves careful interpretation.

**Key words:** IgG4, IgG4-related disease, plasmablast, $^{18}$F-FDG PET/CT, fibrosis

CLINICAL SCIENCE

[1]IRCCS San Raffaele Scientific Institute, Unit of Immunology, Rheumatology, Allergy and Rare Diseases, Milan, [2]Milan, IRCCS San Raffaele Scientific Institute, Università Vita-Salute San Raffaele, [3]Institute of Bioimaging and Molecular Physiology, National Research Council, [4]IRCCS San Raffaele Scientific Institute, Nuclear Medicine, [5]IRCCS San Raffaele Scientific Institute, Unit of Immunohematology, [6]IRCCS San Raffaele Scientific Institute, Pathology Unit, [7]Pancreato-Biliary Endoscopy and Endosonography Division and [8]Division of Pancreatic Surgery, Pancreas Translational and Clinical Research Center, IRCCS San Raffaele Scientific Institute, Milan, Italy

Submitted 21 January 2017; accepted 23 May 2017

*Alvise Berti and Emanuel Della-Torre contributed equally to the study.

Correspondence to: Emanuel Della-Torre, Unit of Immunology, Rheumatology, Allergy and Rare Diseases, IRCCS-San Raffaele Scientific Institute, via Olgettina 60, 20132, Milan, Italy.
E-mail: dellatorre.emanuel@hsr.it

**Rheumatology key messages**

- [$^{18}$F]Fluorodeoxyglucose uptake in IgG4-related disease lesions reflects perturbations of the B cell compartment.
- Positron emission tomography represents a reliable instrument for assessing IgG4-related disease activity.

## Introduction

IgG4-related disease (IgG4-RD) is a systemic fibro-inflammatory condition characterized by a perturbation of the B cell compartment, which ultimately leads to increased production of IgG4 antibodies, and presumably to fibroblast activation [1]. Definitive diagnosis of IgG4-RD requires the demonstration of specific histological features since available biomarkers, including serum IgG4 levels, have demonstrated relevant shortcomings for diagnostic purposes [2, 3].

[$^{18}$F]Fluorodeoxyglucose ($^{18}$F-FDG) PET/CT has been proposed as an additional tool for the diagnostic work-up of IgG4-RD due to the comprehensive overview of organ involvement provided by this imaging technique [4–6]. As opposed to conventional ultrasonography and CT scanning, $^{18}$F-FDG PET/CT can support the diagnosis of IgG4-RD through the identification of typical localizations and the selection of informative biopsy sites [7, 8]. In addition, $^{18}$F-FDG PET/CT has been increasingly used in the follow-up of patients with IgG4-RD for assessing response to immunosuppressive treatments and for monitoring disease relapse [9, 10]. However, despite its progressive diffusion in the management of patients with IgG4-RD, PET/CT findings are considered *bona fide* surrogates of IgG4-RD activity because the immunopathological events responsible for $^{18}$F-FDG uptake in IgG4-RD lesions are largely unknown.

In order to address the potential correlations between $^{18}$F-FDG PET/CT findings and IgG4-RD activity, we quantified the $^{18}$F-FDG uptake of IgG4-RD lesions using accurate quantitative parameters and correlated them with the following validated clinical, serological and immunological biomarkers of IgG4-RD: IgG4-RD Responder Index (RI) [11], CRP, ESR, serum IgG4 levels, circulating plasmablasts and the enhanced liver fibrotic (ELF) score. The level of circulating plasmablasts and the ELF score were used as indicators of B cells and fibroblast activation, respectively, two major immunopathological features of IgG4-RD [12, 13, 14]. Circulating plasmablasts, the precursors of tissue resident antibody secreting plasma cells, are also considered the best currently available biomarker of IgG4-RD activity because they are elevated in patients with untreated IgG4-RD, decline with disease remission and re-emerge during disease flare [12].

## Methods

### Patients

Twenty consecutive patients with active untreated IgG4-RD referred to our tertiary care centre between June 2012 and June 2016 were included in the present observational prospective cohort study. Patients with exclusive lymph node involvement were excluded given the challenging differentiation between reactive and IgG4-RD lymphadenopathy on PET/CT scan. IgG4-RD was diagnosed according to the 'Consensus statement on the pathology of IgG4-RD'; the 'Comprehensive diagnostic criteria for IgG4-RD' were used when tissue biopsies were not available [2, 15]. Patients with pancreatic involvement who did not undergo pancreatic resection were diagnosed with definite IgG4-RD according to the 'International consensus diagnostic criteria for autoimmune pancreatitis' [16]. IgG4-RD activity was assessed by means of the IgG4-RD RI, a tool developed for clinical trials to define active disease (IgG4-RD RI $>3$), disease remission (IgG4-RD RI $<3$ off glucocorticoid therapy) and complete response to immunosuppressive treatments (IgG4RD RI $<3$ on treatment) [11, 17]. All patients gave written informed consent for the analyses performed. The study was conducted according to the Declaration of Helsinki and approved by the Institutional Review Board of San Raffaele Scientific Institute.

### Laboratory analysis

CRP, ESR, total IgG, IgG1, IgG2, IgG3, IgG4 subclasses, ELF score and circulating plasmablasts were measured in all patients prior to any treatment and after immunosuppressive therapy. The ELF score was determined on serum samples by employing the proprietary Conformité Européenne marked assay developed for the ELF test by Siemens Healthcare Diagnostics Inc. (Tarrytown, NY, USA) and was performed on the Advia Centaur platform (Siemens Healthcare Diagnostics Inc., Erlangen, Germany) according to manufacturer's instructions. Flow cytometry was performed on EDTA whole blood samples, using a lyse-no-wash technique (ammonium chloride) and a panel of directly conjugated antibodies (CD19A700-CD20APC-CD27PC7-CD38A750; Navios flow cytometer; Beckman Coulter, Indianapolis, IN, USA). Plasmablasts were defined as CD19$^+$ CD20$^-$ CD38$^+$ brightCD27$^+$ on the CD19$^+$ lymphocytes population gate.

### Imaging studies

Whole-body $^{18}$F-FDG PET scans were performed on the following PET/CT scanners routinely used in the Nuclear Medicine Department of our institute: Discovery ST, Discovery STE, Discovery-690 (General Electric Medical Systems, Milwaukee, WI, USA) and Gemini GXL PET/CT system (Philips Medical Systems, Best, The Netherlands). Patients fasted for 6 h before the intravenous injection of 1 mCi/10 kg of $^{18}$F-FDG. Blood glucose level was measured before injection to ensure euglycaemic glucose metabolism ($<$140 ml/mg). $^{18}$F-FDG PET/CT scans were performed according to the institutional and international guidelines provided by the European Association of Nuclear Medicine [18]. Patients were scanned between the head and thigh with arms down. PET/CT scanners

were cross-calibrated with a dose measurement system and optimized to guarantee the comparability of quantitative PET data. PET images were reconstructed including the corrections for random, scatter and attenuation and analysed both qualitatively and quantitatively. Reconstructed PET images were reviewed by two nuclear medicine physicians and by two immunologists expert in IgG4-RD in order to achieve consensus on IgG4-RD organ involvement. Foci of increased glucose metabolism (i.e. IgG4-RD lesions) were segmented by an automatic technique in order to define a discrete metabolic volume (MV) [19]. Quantitative assessment of the radiotracer uptake within a given MV was then evaluated by means of the mean body-weighted standardized uptake value corrected for partial volume effect (PVC-SUV) and the total lesion glycolysis (TLG) [20]. The IgG4-RD lesion with the highest PVC-SUV was selected for correlation studies in patients with multi-organ involvement. Lesions with a sphere-equivalent diameter $<$1 cm were not considered because of the risk of low quantification accuracy [20]. TLG was calculated for each quantified uptake as the product of mean PVC-SUV and MV by combining volumetric and metabolic information. In order to obtain a surrogate quantitative biomarker of total disease burden, the TLG of each lesion was summed in order to obtain a total TLG for each patient. Total TLG was calculated both excluding ($TLG_{tot-ln}$) and including ($TLG_{tot+ln}$) lymph nodes. The $^{18}$F-FDG-PET/CT scan was repeated in 10 patients to assess disease activity after immunosuppressive treatment.

### Statistical analysis

Variables are presented as median and interquartile range for serological and immunological biomarkers and FDG-PET measurements, unless otherwise specified. Prism version 6.00 was utilized for statistical analysis (GraphPad Software, La Jolla, CA, USA). Categorical variables were compared using Fisher's exact test. Normally and non-normally distributed variables were compared using Student's t-test and the Mann–Whitney U-test, respectively. Parametric correlations were calculated using Spearman's correlation test. $P < 0.05$ was considered statistically significant.

## Results

### Clinical, serological and immunological features of the patient cohort at baseline

Twenty patients (13 males, 7 females) with a mean age of 61 years (range, 30–78 years) were included in the study (Table 1). Twelve patients with available histological examination were diagnosed as definite IgG4-RD according to the 'Consensus statement on the pathology of IgG4-RD' [2] and the 'Comprehensive diagnostic criteria for IgG4-RD' [15]. Four patients without available tissue biopsies but with characteristic pancreatic involvement were diagnosed as definite IgG4-RD according to the 'International consensus diagnostic criteria for autoimmune pancreatitis' [16]. One patient with available histology but normal serum IgG4 levels was diagnosed as probable IgG4-RD according to the 'Comprehensive diagnostic criteria for IgG4-RD' [15]. Three patients without available biopsies were diagnosed as possible IgG4-RD according to the 'Comprehensive diagnostic criteria for IgG4-RD' [15]. The aorta and/or its major branches was the most commonly affected organ (seven cases), followed by the pancreas (five cases), lung, orbits, parotid and submandibular glands (three cases each), paranasal sinuses, palate, bone and lacrimal glands (two cases each). The meninges, thyroid and skin were involved in one case each. Thirteen (65%) patients had two or more organs affected by IgG4-RD. All patients had active IgG4-RD as defined by a median IgG4-RD RI value of 9 (range, 6–15; normal $<$3). The median levels of ESR, CRP, serum IgG4, plasmablasts and ELF score were 19 mm/h (range, 4–121 mm/h, normal $<$20 mm/h), 4.3 mg/l (range 0.0–48.0 mg/l; normal $<$6 mg/l), 308 mg/dl (range, 80–2100 mg/dl, normal $<$135 mg/dl), 2270 cells/ml (range, 130–40 840 cells/ml, normal $<$650 cells/ml) and 8.9 (range, 7.2–12.1, normal $<$7.7), respectively. ESR, CRP, serum IgG4 levels, plasmablasts and ELF score were elevated in 9 (45%), 7 (35%), 17 (85%), 17 (85%) and 11 (55%) patients, respectively.

### Quantitative $^{18}$F-FDG PET/CT findings at baseline

$^{18}$F-FDG PET/CT scan evaluations identified 46 anatomical sites of possible IgG4-RD involvement in the 20 studied patients, with a median of 2 sites per patient (range, 1–6). IgG4-RD affected organs with the maximum PVC-SUV value were the aorta (six patients), the parotid glands (three patients), the lacrimal glands, the lungs and the pancreas (two patients each), submandibular glands, bone, orbits, meninges and thyroid (one patient each). Eight patients (40%) had evidence of lymph node involvement (Table 1 and Fig. 1). The mean PVC-SUV value of the most metabolically active IgG4-RD lesions was 7.63 g/cc (4.81–10.57g/cc). The highest PVC-SUV value was measured in a patient with thyroid involvement. The maximum $TLG_{tot+ln}$ was measured in a patient with aortic and lymph nodes involvement (Table 1). In general, the highest values of TLG were described when the aorta was involved. $TLG_{tot+ln}$ and $TLG_{tot-ln}$ values were 318.50 g (148.71–520.96 g) and 254.25 g (128.70–469.91 g), respectively. Lymph node involvement, systemic *vs* localized disease, and the number of organs involved did not influence $TLG_{tot-ln}$ and $TLG_{tot+ln}$ values ($P > 0.05$ in all comparisons; supplementary Fig. S1, available at *Rheumatology* Online).

### Correlation studies between $^{18}$F-FDG PET/CT uptake, clinical, serological and immunological biomarkers at baseline

No statistically significant correlation was found between the PVC-SUV value of the most metabolically active IgG4-RD lesion and IgG4-RD RI, CRP, ESR, serum IgG4 levels and ELF score ($P > 0.05$ for all the comparisons; supplementary Fig. S2A, available at *Rheumatology* Online). A statistically significant positive correlation was found between the PVC-SUV of the most metabolically

**Table 1** Clinical, serological, immunological and radiological findings of the patient cohort at baseline

| Patient no.[a] | Organ involvement | Diagnosis | IgG4-RD RI < 3 | ESR <20 mm/h | CRP <6 mg/l | Serum IgG4 <135 mg/dl | Plasmablast 0–650 cells/ml | ELF score <7.7 | PVC-SUV[b], g/cc | $TLG_{tot+ln}$, g | $TLG_{tot-ln}$, g |
|---|---|---|---|---|---|---|---|---|---|---|---|
| 1 | Aorta and its branches | D | 9 | 38 | 14.0 | 420 | 1000 | 9.8 | 2.78 (aorta) | 252.48 | 252.48 |
| 2 | Aorta and its branches, meninges | Pr | 9 | 43 | 8.3 | 106 | 2000 | — | 8.85 (meninges) | 286.78 | 286.78 |
| 3 | Skin, lymph nodes, lacrimal glands, paranasal sinuses | D | 15 | 64 | 0.0 | 2100 | 10 000 | 9.7 | 10.91 (lacrimal) | 367.58 | 40.62 |
| 4 | Paranasal sinuses, palate, orbits, bone | D | 12 | 30 | 48.0 | 151 | 4780 | 7.6 | 8.60 (bone) | 127.19 | 127.19 |
| 5 | Lymph nodes, parotid gland | D | 9 | 4 | 2.8 | 973 | 9330 | 8.5 | 7.24 (parotid) | 528.54 | 165.70 |
| 6 | Aorta | D | 6 | 37 | 8.0 | 178 | 130 | 8.8 | 4.07 (aorta) | 570.81 | 570.81 |
| 7 | Orbits, lymph nodes, lung | D | 12 | 16 | 4.3 | 286 | 40840 | 7.5 | 9.54 (lung) | 334.68 | 331.02 |
| 8 | Pancreas, lymph nodes | D | 9 | 20 | 1.3 | 221 | 3560 | 9.0 | 4.25 (pancreas) | 155.92 | 94.83 |
| 9 | Lymph nodes, palate, orbits, lung, bone, submandibular glands | D | 9 | 5 | 0.3 | 421 | 5650 | 7.4 | 11.68 (orbit) | 302.31 | 158.36 |
| 10 | Aorta and its branches | P | 9 | 53 | 14.0 | 363 | 1980 | — | 3.31 (aorta) | 381.70 | 381.70 |
| 11 | Aorta and its branches, lymph nodes | P | 9 | 6 | 3.3 | 185 | 1370 | — | 7.25 (aorta) | 3479.7 | 3316.90 |
| 12 | Pancreas, lung, lymph nodes | D | 12 | 121 | 46.3 | 343 | 5400 | 9.5 | 8.13 (lung) | 465.45 | 256.02 |
| 13 | Thyroid, pancreas | D^ | 9 | 6 | 0.0 | 308 | 4000 | 12.1 | 39.34 (thyroid) | 91.37 | 91.37 |
| 14 | Aorta and its branches | D | 6 | — | — | — | 380 | 8.6 | 6.98 (aorta) | 295.44 | 295.44 |
| 15 | Aorta | P | 9 | 48 | — | 173 | 1030 | 7.6 | 30.21 (aorta) | 692.09 | 692.09 |
| 16 | Lymph nodes, parotid glands | D | 9 | 15 | 10.1 | 257 | 5130 | 7.2 | 8.01 (parotid) | 118.91 | 113.87 |
| 17 | Pancreas, subandibular glands | D^ | 6 | 6 | 1.8 | 156 | 810 | 9.5 | 5.43 (submandibular) | 133.24 | 133.24 |
| 18 | Pancreas, submandibular and lacrimal glands | D^ | 12 | 10 | 4.9 | 1120 | 2020 | 9.8 | 13.28 (lacrimal) | 548.25 | 548.25 |
| 19 | Parotid glands, aorta, pancreas | D^ | 15 | 19 | 0.8 | 498 | 2520 | 9.1 | 4.60 (parotid) | 146.30 | 146.30 |
| 20 | Pancreas | D | 6 | 7 | — | 586 | 940 | — | 6.67 (pancreas) | 499.31 | 499.31 |

[a]Patients cohort includes 13 males and 7 females with a mean age of 61 years (range, 30–78 years). [b]PVC-SUV values refer to IgG4-RD lesion showing the highest avidity for $^{18}$F-FDG reported in parentheses. D: definite IgG4-RD according to the 'Consensus statement on the pathology of IgG4-RD' [2] and to the 'Comprehensive diagnostic criteria for IgG4-RD' [15] when biopsy was available; D^: definite IgG4-RD according to the 'International consensus diagnostic criteria for autoimmune pancreatitis' [16] when biopsy was not available but pancreatic involvement was characteristic of type 1 autoimmune pancreatitis; ELF: enhanced liver fibrosis score; IgG4-RD RI: IgG4-related disease Responder Index; P: possible IgG4-RD according to the 'Comprehensive diagnostic criteria for IgG4-RI' [15] when biopsy was not available; Pr: probable IgG4-RD according to the 'Comprehensive diagnostic criteria for IgG4-RD' [15] when biopsy was available but serum IgG4 were <135 mg/dl; PVC-SUV: standardized uptake value corrected for partial volume effect; TLG: total lesion glycolysis with lymph nodes ($TLG_{tot+ln}$) and without lymph nodes ($TLG_{tot-ln}$).

FIG. 1 Representative $^{18}$F-FDG PET/CT findings in our cohort of patients with IgG4-related disease at baseline

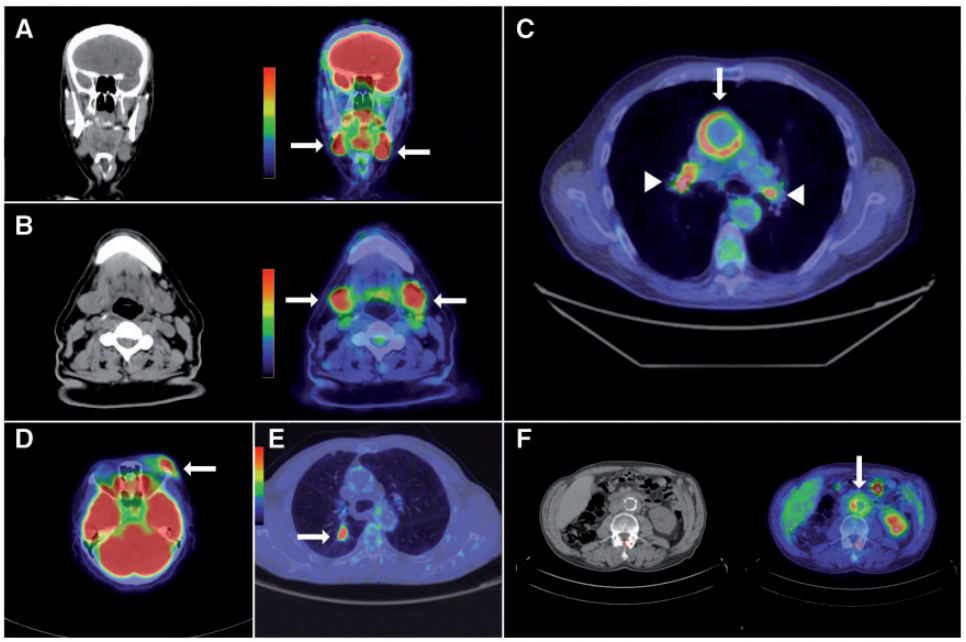


(**A** and **B**) Submandibular gland involvement in patient 17 (arrows); (**C**) thoracic aorta (arrow) and hilar lymph node (arrowheads) involvement in patient 11; (**D**) left lacrimal gland involvement in patient 3 (arrow); (**E**) isolated lung nodule in patient 7 (arrow); (**F**) abdominal aorta involvement in patient 10 (arrow)—all showing intense $^{18}$F-FDG uptake at baseline.

active IgG4-RD lesion and the levels of circulating plasmablasts ($r = 0.49$, $P < 0.05$) (Fig. 2). No statistically significant correlation was found between either $TLG_{tot+ln}$ or $TLG_{tot-ln}$ values and IgG4-RD RI, CRP, ESR, serum IgG4 levels and ELF score ($P > 0.05$ for all the comparisons; supplementary Fig. S2B and C, available at *Rheumatology* Online). Circulating plasmablasts count did not correlate with $TLG_{tot+ln}$ ($P > 0.05$) but inversely correlated with $TLG_{tot-ln}$ ($r = 0.50$, $P < 0.05$; Fig. 2).

### Quantitative $^{18}$F-FDG PET/CT findings after immunosuppressive therapy

Ten patients underwent a second $^{18}$F-FDG PET/CT scan after a median of 5.5 months (range, 2–7 months) of immunosuppressive therapy (Table 2). Seven of them were initially treated with oral prednisone (0.5–1 mg/kg) according to the 'International consensus guidance statement on the treatment of IgG4-RD' [21]; prednisone was then gradually tapered over a period of 6 months. Two patients were also treated with rituximab (2 i.v. infusions of 1000 mg 15 days apart), and three with oral or s.c. MTX (15–20 mg/week). Three patients were treated with MTX alone.

At the time of the second $^{18}$F-FDG PET/CT scan, seven patients were still on glucocorticoids; all of them but patient 3 were on oral prednisone $\leqslant$5 mg/day; patient 3 was on 10 mg/day. Three patients were on MTX alone. All 10 patients were on complete response (i.e. an IgG4-RD RI < 3 on treatment) and showed a consensual reduction of circulating plasmablasts, PVC-SUV, $TLG_{tot+ln}$ and $TLG_{tot-ln}$ (Table 2 and Fig. 3). The median value of circulating plasmablasts dropped from 2270 cells/ml (range, 130–40840 cells/ml) at baseline to 300 cells/ml (range, 0–3610 cells/ml).

The median PVC-SUV calculated on the same IgG4-RD lesions considered for pre-treatment analyses decreased from 7.69 g/cc (4.29–9.88 g/cc) at baseline to 0 g/cc (0–5.98 g/cc) ($P < 0.05$). The median $TLG_{tot+ln}$, and $TLG_{tot-ln}$ values decreased from 351.13 g (153.52–506.62 g) and 210.86 g (123.64–373.10 g) at baseline to 23.96 g (0–240.57 g) ($P < 0.05$) and 23.96 g (0–67.27 g) ($P < 0.05$), respectively. The mean percentage reduction of PVC-SUV, $TLG_{tot+ln}$ and $TLG_{tot-ln}$ values compared with baseline was 63 ± 50%, 75 ± 37% and 77 ± 28%, respectively (Fig. 2). Despite the decrease of circulating plasmablast counts and TLG values after immunosuppressive treatment, PVC-SUV values of the lacrimal gland in patient 3 and of a lung lesion in patient 12 increased from 10.91 to 13.45 g/cc and from 8.31 to 10.74 g/cc, respectively (Fig. 3). TLG values in patient 5 increased from 528.54 to 621.21 g when lymph nodes were included in the measurement ($TLG_{tot+ln}$), and decreased from 165.70 to 115.02 g when lymph nodes were excluded ($TLG_{tot-ln}$) (Table 2 and Fig. 3).

## Discussion

$^{18}$F-FDG PET/CT is increasingly considered an ideal imaging technique for the evaluation of IgG4-RD because it appears to offer a comprehensive overview of disease extension and response to immunosuppressive treatments

**Fig. 2** Correlation between $^{18}$F-FDG PET/CT parameters and immunological biomarkers of IgG4-related disease activity

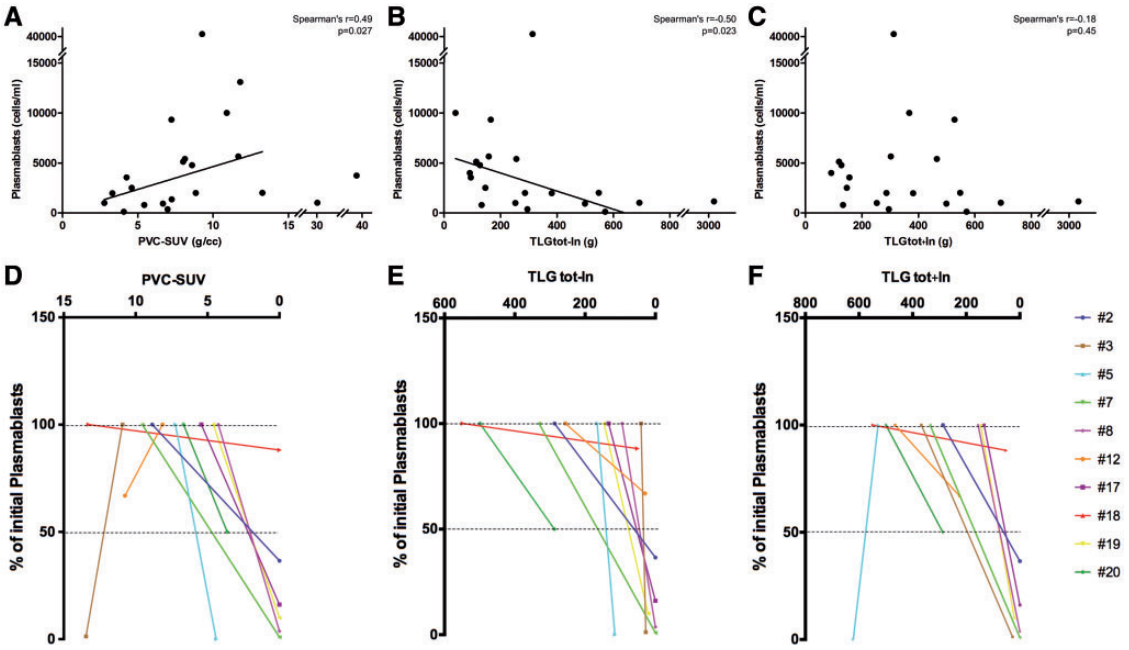


At baseline, (**A**) PVC-SUV of the most highly active IgG4-RD lesion positively correlates with the number of circulating plasmablasts ($r = 0.49$, $P = 0.027$); (**B**) $TLG_{tot-In}$ inversely correlates with circulating plasmablast levels ($r = 0.50$, $P = 0.023$); (**C**) $TLG_{tot+In}$ does not correlate with circulating plasmablast levels ($P > 0.05$). Consensual reduction of circulating plasmablasts and PVC-SUV (**D**), $TLG_{tot-In}$ (**E**) and $TLG_{tot+In}$ (**F**) after complete response induced by immunosuppressive therapies in 10 patients. Reduction of circulating plasmablasts is expressed as percentage of their initial number at baseline.

**Table 2** Plasmablast counts and quantitative $^{18}$F-FDG PET/CT findings after immunosuppressive therapy

| Patient no. | Therapy | Duration of therapy[a], months | IgG4-RD RI (<3) | Plamablasts, cells/ml | PVC-SUV[b], g/cc | $TLG_{tot+In}$, g | $TLG_{tot-In}$, g |
|---|---|---|---|---|---|---|---|
| 2 | PDN + MTX | 4 | 2 | 730 | 0 | 0 | 0 |
| 3 | PDN + RTX | 2 | 1 | 120 | 13.45 | 27.44 | 27.44 |
| 5 | MTX | 7 | 1 | 0 | 4.40 | 621.21 | 115.02 |
| 7 | mPDN + RTX + PDN | 6 | 0 | 350 | 0 | 0 | 0 |
| 8 | PDN + MTX | 5 | 2 | 130 | 0 | 0 | 0 |
| 12 | PDN | 6 | 2 | 3610 | 10.74 | 224.92 | 29.57 |
| 17 | PDN | 4 | 1 | 130 | 0 | 0 | 0 |
| 18 | PDN + MTX | 4 | 2 | 1780 | 0 | 51.35 | 51.35 |
| 19 | MTX | 6 | 1 | 250 | 0 | 20.47 | 20.47 |
| 20 | MTX | 6 | 2 | 470 | 3.63 | 287.50 | 287.50 |

[a]Duration of therapy also represents the time frame between the baseline and the follow-up $^{18}$F-FDG PET/CT scan. At the time of the follow-up PET/CT scan, seven patients were on glucocorticoids; all of them except patient 3 were on PDN $\leqslant$ 5 mg/day; patient 3 was on PDN 10 mg/day. [b]PVC-SUV of the IgG4-RD lesion showing the highest avidity for $^{18}$F-FDG for each patient. PVC-SUV values refer to the IgG4-RD lesion indicated in parentheses in Table 1. IgG4-RD RI: IgG4-related disease Responder Index; mPDN: i.v. metilprednisolone 1 g for 3 consecutive days; MTX: oral or s.c. MTX 15–20 mg/week; PDN: oral prednisone (0.6–1 mg/kg tapered in 6 months); PVC-SUV: standardized uptake value corrected for partial volume effect; RTX: rituximab (2 i.v. 1000 mg infusions 15 days apart); TLG: total lesion glycolysis with lymph nodes ($TLG_{tot+In}$) and without lymph nodes ($TLG_{tot-In}$).

[4–10]. The immunopathological events that sustain $^{18}$F-FDG uptake in IgG4-RD lesions, however, are still largely unexplored and a clear relationship between PET/CT findings and IgG4-RD activity remains elusive. Available studies, in fact, address these important issues only marginally because the majority of them evaluate IgG4-RD burden and response to treatments by means of qualitative rather than quantitative $^{18}$F-FDG PET/CT parameters

FIG. 3 Representative $^{18}$F-FDG PET/CT findings in our cohort of patients with IgG4-related disease after treatment

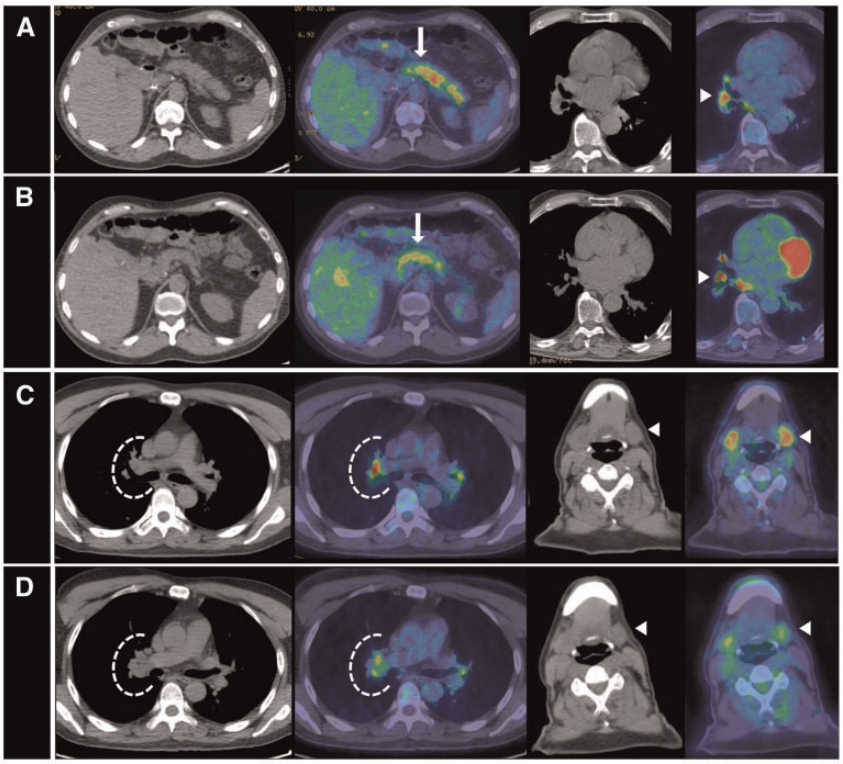


(**A**) Pancreatic (sausage like) enlargement (arrow) and lung nodules (arrowhead) in patient 12 showing intense $^{18}$F-FDG uptake at baseline. (**B**) Volumetric and metabolic response of the pancreas in patient 12 after treatment (arrow); increased $^{18}$F-FDG uptake of the lung nodules in patient 12 after treatment (arrowheads). (**C**) Hilar lymph nodes (circle) and submandibular glands (arrowheads) in patient 5 showing $^{18}$F-FDG uptake at baseline. (**D**) Volumetric increase and metabolic response of the hilar lymph nodes in patient 5 after treatment (circle); volumetric and $^{18}$F-FDG uptake reduction of the submandibular glands in patient 5 after treatment (arrowhead).

[4–10]. In addition, those studies are retrospective and often analyse data from multi-centric cohorts of patients obtained on different PET/CT scanners [4–10].

A major novelty of our study is represented by the assessment of IgG4-RD activity using two quantitative $^{18}$F-FDG PET/CT biomarkers: PVC-SUV and TLG. As opposed to other PET/CT biomarkers adopted in previous studies such as $SUV_{max}$ and $SUV_{mean}$ [7, 9], SUV and TLG with partial volume correction offer more reliable metabolic information and more accurate quantification of $^{18}$F-FDG uptake because they are less influenced by the dimension of the target lesion. This bias is known as the partial volume effect and is thought to underestimate up to 80% of the real $^{18}$F-FDG uptake [19–24].

In the present work we correlate validated clinical and serological biomarkers of IgG4-RD activity with quantitative $^{18}$F-FDG PET/CT parameters, and demonstrate that $^{18}$F-FDG uptake of IgG4-RD lesions likely reflects immunological perturbations of the B cell compartment rather than processes related to fibroblast activation and extracellular matrix deposition. In particular, we show that the levels of circulating plasmablasts positively correlate with PVC-SUV suggesting that $^{18}$F-FDG uptake in IgG4-RD lesions may depend, at least in part, on plasmablasts migration into inflamed tissues. Interestingly, circulating plasmablasts inversely correlated with TLG values calculated excluding lymph nodes ($TLG_{tot-ln}$) but did not correlate with TLG values when lymph nodes were included in the assessment of disease burden ($TLG_{tot+ln}$). This result might be due to the inclusion of reactive lymph nodes in the measurement of $TLG_{tot+ln}$ and, thus, to overestimation of the real systemic IgG4-RD involvement. Reactive and IgG4-RD lymph nodes, in fact, are indistinguishable on the basis of the sole $^{18}$F-FDG PET/CT findings, an aspect that complicates the interpretation of PET/CT results and the overall assessment of disease extent.

The concomitant reduction of circulating plasmablasts, PVC-SUV and TLG values with disease improvement further supports the close relationship between PET/CT findings and B cell activation. In addition, the decrease of quantitative $^{18}$F-FDG PET parameters together with clinical remission demonstrates the reliability of PET/CT imaging in evaluating IgG4-RD activity and response to immunosuppressive therapies. However, it is noteworthy that the PVC-SUV of the most metabolically active IgG4-RD lesion in patients 3 and 12 increased despite clinical improvement, reduction of circulating plasmablasts counts and decrease

of TLG values. Similar clinical–radiological discrepancies are frequently encountered in oncological settings, and occur when both metabolic and volumetric PET/CT parameters of neoplastic lesions are not modified accordingly in response to chemotherapy [25]. This was indeed a major concern while assessing IgG4-RD activity on PET/CT scan after treatment. In particular, common confounding scenarios stemmed from the appearance of novel lymph nodes with high $^{18}$F-FDG uptake, typically in the mediastinum or abdomen; increased or persistent $^{18}$F-FDG uptake in pre-existing lymph nodes; increased or persistent $^{18}$F-FDG uptake in organs showing dimensional improvement; and decreased $^{18}$F-FDG uptake in organs showing volumetric increase. In addition, TLG values showed different responses to treatment depending on whether lymph nodes were included in the measurement (Table 2). In patient 5, for example, increased volume and $^{18}$F-FDG uptake of mediastinal lymph nodes led to an increase of $TLG_{tot+ln}$ despite improvement of parotid glands enlargement and reduction of PVC-SUV values.

Taken together, these results add substantial insights to the interpretation of $^{18}$F-FDG PET/CT findings in patients with IgG4-RD. First, we show that quantitative PET/CT scan parameters of $^{18}$F-FDG uptake reflect circulating plasmablast expansion, the best currently available biomarker of IgG4-RD activity [12]. Second, we show that these quantitative PET/CT parameters can be used for longitudinally following the response to immunosuppression. Third, we describe how volumetric and metabolic responses of IgG4-RD lesions in the same patient might differ after immunosuppressive treatment, thus complicating the interpretation of residual disease activity in the case of multiple organ involvement. Finally, our results indicate that lymph nodes represent a confounding variable in the assessment of the overall IgG4-RD burden since PET/CT studies cannot discriminate between reactive and IgG4-RD lymph nodes. A close collaboration between clinicians and nuclear medicine specialists is, therefore, necessary to interpret $^{18}$F-FDG PET/CT findings in IgG4-RD patients and to avoid over- or underestimation of IgG4-RD burden.

Other routinely used IgG4-RD biomarkers such as serum IgG4 and IgG4-RD RI did not correlate with $^{18}$F-FDG uptake of IgG4-RD lesions, further confirming the shortcomings of both parameters for the assessment of IgG4-RD activity [3, 16]. Indeed, the current IgG4-RD RI algorithm strictly depends on the value of serum IgG4, a biomarker of poor accuracy by itself [11]. Eventually, we did not find any correlation between $^{18}$F-FDG uptake and the ELF score, a recently validated biomarker of systemic fibrosis [13], suggesting that PET/CT may not be an ideal imaging technique for obtaining clues about fibroblast activation and processes related to collagen deposition.

These results are supported by a number of significant strengths. First, this is a monocentric prospective study designed to correlate IgG4-RD activity with the most accurate biomarkers of $^{18}$F-FDG uptake. In addition, our study cohort is derived from one of the largest single centre cohorts of IgG4-RD patients, an aspect that ensured uniform inclusion criteria and follow-up [26]. Furthermore, $^{18}$F-FDG PET/CT data were obtained on cross-calibrated PET/CT scanners, thus allowing more reliable comparisons between patients, before and after treatment. Our work has also some limitations. Despite a thorough quantitative analysis, in fact, the FDG-PET/CT scan is inherently unable to differentiate reactive from pathological lymph nodes and, thus, to unequivocally define IgG4-RD burden, especially in patients with multi-organ involvement. In addition, although our results correlate circulating plasmablasts and $^{18}$F-FDG uptake in IgG4-RD lesions, a full comprehension of the immunopathological events sustaining PET/CT findings in this condition would require further correlation studies between imaging and pathological features. Finally, we recognize that more robust information could have been obtained from a larger cohort of patients; however, we decided to limit our analysis to 20 subjects who had laboratory tests and PET/CT scan performed on the same day in order to extrapolate more reliable correlations.

In conclusion, we present the first systematic analysis of the relationship between PET/CT scan findings and IgG4-RD activity by correlating quantitative biomarkers of $^{18}$F-FDG uptake and IgG4-RD. Thanks to this systematic approach we have unveiled the immunological basis for considering PET/CT a reliable instrument for assessing IgG4-RD activity. In addition, the evidence that PET/CT parameters reflect perturbations of the B cell compartment provides a solid rationale for further studies aiming to understand whether $^{18}$F-FDG PET/CT can be used to predict response to B cell depletion therapy.

*Funding*: This work was supported by the 'Fondazione Italiana per la Ricerca sull'Artrite' (FIRA Onlus 2014) and by the 'Collegio Ghislieri' (Pavia).

*Disclosure statement*: The authors have declared no conflicts of interest.

## Supplementary data

Supplementary data are available at *Rheumatology* Online.

## References

1 Della-Torre E, Lanzillotta M, Doglioni C. Immunology of IgG4-related disease. Clin Exp Immunol 2015;181:191–206.

2 Deshpande V, Zen Y, Chan JK *et al*. Consensus statement on the pathology of IgG4-related disease. Mod Pathol 2012;25:1181–92.

3 Carruthers MN, Khosroshahi A, Augustin T, Deshpande V, Stone JH. The diagnostic utility of serum IgG4 concentrations in IgG4-related disease. Ann Rheum Dis 2015;74:14–8.

4 Tokue A, Higuchi T, Arisaka Y *et al*. Role of F-18 FDG PET/CT in assessing IgG4-related disease with inflammation of head and neck glands. Ann Nucl Med 2015;29:499–505.

5 Ebbo M, Grados A, Guedj E *et al*. Usefulness of 2-[$^{18}$F]-fluoro-2-deoxy-D-glucose-positron emission tomography/

computed tomography for staging and evaluation of treatment response in IgG4-related disease: a retrospective multicenter study. Arthritis Care Res 2014;66:86–96.

6 Nakatani K, Nakamoto Y, Togashi K. Utility of FDG PET/CT in IgG4-related systemic disease. Clin Radiol 2012;67:297–305.

7 Zhao Z, Wang Y, Guan Z *et al*. Utility of FDG-PET/CT in the diagnosis of IgG4-related diseases. Clin Exp Rheumatol 2016;34:119–25.

8 Lee J, Hyun SH, Kim S *et al*. Utility of FDG PET/CT for differential diagnosis of patients clinically suspected of IgG4-related disease. Clin Nucl Med 2016;41:e237–43.

9 Zhang J, Chen H, Ma Y *et al*. Characterizing IgG4-related disease with $^{18}$F-FDG PET/CT: a prospective cohort study. Eur J Nucl Med Mol Imaging 2014;41:1624–34.

10 Nakatsuka Y, Handa T, Nakamoto Y *et al*. Total lesion glycolysis as an IgG4-related disease activity marker. Mod Rheumatol 2015;25:579–84.

11 Carruthers MN, Stone JH, Deshpande V, Khosroshahi A. Development of an IgG4-RD Responder Index. Int J Rheumatol 2012;2012:259408.

12 Wallace ZS, Mattoo H, Carruthers M *et al*. Plasmablasts as a biomarker for IgG4-related disease, independent of serum IgG4 concentrations. Ann Rheum Dis 2015;74:190–5.

13 Mattoo H, Mahajan VS, Della-Torre E *et al*. De novo oligoclonal expansions of circulating plasmablasts in active and relapsing IgG4-related disease. J Allergy Clin Immunol 2014;134:69–87.

14 Della-Torre E, Feeney E, Deshpande V *et al*. B-cell depletion attenuates serological biomarkers of fibrosis and myofibroblast activation in IgG4-related disease. Ann Rheum Dis 2015;74:2236–43.

15 Umehara H, Okazaki K, Masaki Y *et al*. Comprehensive diagnostic criteria for IgG4-related disease (IgG4-RD), 2011. Mod Rheumatol 2012;22:21–30.

16 Shimosegawa T, Chari ST, Frulloni L *et al*. International consensus diagnostic criteria for autoimmune pancreatitis: guidelines of the International Association of Pancreatology. Pancreas 2011;40:352–8.

17 Carruthers MN, Topazian MD, Khosroshahi A *et al*. Rituximab for IgG4-related disease: a prospective, open-label trial. Ann Rheum Dis 2015;74:1171–7.

18 Boellaard R, O'Doherty MJ, Weber WA *et al*. FDG PET and PET/CT: EANM procedure guidelines for tumour PET imaging: version 1.0. Eur J Nucl Med Mol Imaging 2010;37:181–200.

19 Gallivanone F, Interlenghi M, Canevari C, Castiglioni I. A fully automatic, threshold-based segmentation method for the estimation of the Metabolic Tumor Volume from PET images: Validation on 3D printed anthropomorphic oncological lesions. J Instrum 2016;11:C01022.

20 Gallivanone F, Stefano A, Grosso E *et al*. PVE correction in PET-CT whole-body oncological studies from PVE-affected images images. IEEE Transact Nuclear Sci 2011;58:736–47.

21 Hoetjes NJ, van Velden FH, Hoekstra OS *et al*. Partial volume correction strategies for quantitative FDG PET in oncology. Eur J Nucl Med Mol Imaging 2010;37:1679–87.

22 Stefano A, Gallivanone F, Messa C, Gilardi MC, Gastiglioni I. Metabolic impact of partial volume correction of [$^{18}$F]FDG PET-CT oncological studies on the assessment of tumor response to treatment. Q J Nucl Med Mol Imaging 2014;58:413–23.

23 Gallivanone F, Canevari C, Gianolli L *et al*. A partial volume effect correction tailored for $^{18}$F-FDG-PET oncological studies. Biomed Res Int 2013;2013:780458.

24 Soret M, Bacharach SL, Buvat I. Partial-volume effect in PET tumor imaging. J Nucl Med 2007;48:932–45.

25 Young H, Baum R, Cremerius U *et al*. Measurement of clinical and subclinical tumour response using [$^{18}$F]-fluorodeoxyglucose and positron emission tomography: review and 1999 EORTC recommendations. European Organization for Research and Treatment of Cancer (EORTC) PET Study Group. Eur J Cancer 1999;35:1773–82.

26 Campochiaro C, Ramirez GA, Bozzolo EP *et al*. IgG4-related disease in Italy: clinical features and outcomes of a large cohort of patients. Scand J Rheumatol 2016;45:135–45.